NJC

Accepted Manuscript

Volume 1 | Number 1 | Jan 2013 | Pages 1–100

NJC

New Journal of Chemistry
www.rsc.org/njc

A journal for new directions in chemistry

ROYAL SOCIETY OF CHEMISTRY

cnrs

ROYAL SOCIETY OF CHEMISTRY

www.rsc.org/njc

Journal Name

ARTICLE

Structure-properties relationship in diketopyrrolopyrrole based small molecules using functional terminal side chains via direct arylation: a joint experimental and theoretical study

B. Sambathkumar,[ab] P. Shyam Vinod Kumar,[ab] K. Saurav,[c] S. Sundar Kumar Iyer,[c] V. Subramanian,[ab] and N. Somanathan*[ab]

In this article, we report a series of diketopyrrolopyrrole based donor – acceptor small molecules PDPP-OC8, PDPP-EC8, PDPP-EG and PDPP-CNEC8, with different phenyl containing flexible terminal side chains such as alkoxy (-OC$_8$H$_{17}$), ester ((-CO)OC$_8$H$_{17}$), ester with glycol ((-CO)(O(C$_2$H$_4$O)$_3$-CH$_3$)) and cyano acrylate with octyl side chain ((-CN)(CO)OC$_8$H$_{17}$) respectively via direct arylation. A comparative analysis has been done on their opto-electronic properties such as absorption, HOMO, LUMO, band gap, thermal properties, packing nature and hole mobility. The physical properties of the four small molecules were studied using absorption spectroscopy, thermal gravimetric analysis, cyclic voltammetry, differential scanning calorimetry and charge carrier mobility measurements. In comparison to molecules with alkoxy terminal side chain, those with ester and cyano acrylate terminal side chains exhibit (i) low optical band gap from 1.65 eV (alkoxy) to 1.43 eV (ester) (ii) broad absorption covering solar spectrum from 500 to 800 nm. From the results we are able to conclude that the terminal side chains significantly alter their optical and electronic properties. Density functional theory calculations have been carried out to substantiate the opto-electronic characteristics and further understand the effect of terminal alkyl chains.

1. Introduction

Over the last two decades organic photovoltaics (OPVs) based on solution processed bulk heterojunction (BHJ) comprised of polymer/fullerene blends have been of much attraction to research community because of their unique advantages such as low cost, light weight, flexibility and large area device fabrication using various printing methodology.[1] Even though impressive power conversion efficiencies (PCE) over 10% in single junction and 11% in tandem device have been realized in polymer based donor materials, their batch to batch variation in molecular weight, polydisperse nature and purity can lead to variation in their processing properties and device performances.[2] In contrast to polymers, small molecular donor materials are highly attractive owing to their monodisperse nature, definite molecular structure, specific molecular weight, excellent purity and less batch to batch variation.[3] Inspiring success in their power conversion efficiencies over 10% in single layer has been reported based on small molecules as donor materials.[4] Among various small molecular organic semiconductors, thiophene flanked diketopyrrolopyrrole

(DPP) based materials have received more interest in organic solar cells. Their well conjugated fused aromatic frame work favors strong π-π interaction, good absorption in visible range and their electron deficient lactam groups make DPP a strong acceptor. Combining DPP with a variety of donor materials, offers development of wide range of push–pull or donor–acceptor (D–A) systems. These systems exhibit low band gap due to intramolecular charge transfer between donor and the acceptor.[5] In general, such type of D-A systems can be effectively built using traditional cross coupling methodologies like Suzuki, Negishi, Stille, etc. The main drawback of cross coupling is that it needs an organometallic precursor such as organoboron or organotin components which require multi steps for monomer synthesis, expensive purification and release toxic byproducts during coupling. Recently a new technique named direct arylation, alternate to traditional cross coupling methodologies has emerged as a convenient tool for synthesizing organic conjugated material. The advantages of direct arylation are simplicity of reactant and absence of organometallic precursor which makes it as cheap, time effective and environmentally benign.[6] Recently Welch and coworkers reported a series of DPP based small molecules with different end groups and demonstrated that α-C–H bonds of thiophene-DPP can be subjected to direct arylation using palladium catalysis.[7,8] Thus DPP flanked thiophene segment should be the perfect candidate for the study of direct arylation.[9] However, in contrast to polymer, small molecule based semiconductor suffers unsatisfactory film formation and poor morphology because of their inherent crystalline nature which results low device performance. This can be overcome by elegant molecular design and by controlling the side chain engineering.[10]

[a.] CSIR -Central Leather Research Institute, (CSIR)-CLRI, Adyar, Chennai-600 020, India. E-mail: nsomanathan@rediffmail.com; Fax: +91-44-24911589; Tel: +91-44-24437189.
[b.] CSIR-Network of Institutes for Solar Energy, India.
[c.] Department of Electrical Engineering, Indian Institute of Technology Kanpur, Kanpur 208 016, Uttar Pradesh, India
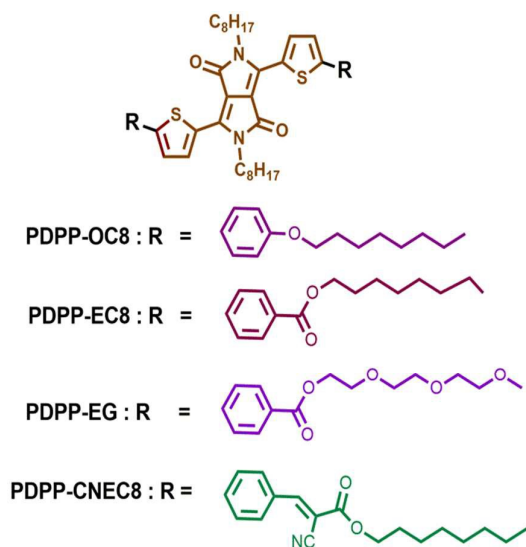
ARTICLE

Journal Name

Figure 1. Chemical structure of four small molecules.

Selecting a rigid conjugated backbone helps in enhancing π-π interaction and also favors solid packing. Apart from using side chains for solubility purpose, recent study reveals that it has an ability to control absorption, emission, HOMO, LUMO, band gap, morphology and molecular packing. On the other hand, there is no appropriate protocol for selecting this flexible side chain.[11] Therefore, designing a donor material with proper side chain with appropriate length and functional group are the key factors for controlling their crystalline nature, solubility, miscibility and orientation of small molecules in thin film which in turn control the charge separation and charge transport properties. Herein, we report four different solution processed small molecules as donor material via direct arylation, with chromophoric thiophene flanked DPP moiety bonded to phenyl group containing various flexible terminal side chains. The effect of different functional flexible side chains in the optical property, band gap, packing nature, HOMO and LUMO energy levels of the four small molecules has been investigated in detail. To gain in-depth understanding of the opto-electronic profiles of the four small molecules, theoretical calculations have been carried out using Density Functional Theory (DFT). [12]

2. Experimental Section

2.1 Materials

2,5-dioctyl-3,6-di(thiophen-2-yl)pyrrolo[3,4-c]pyrrole-1,4(2H,5H)-dione was prepared, according to the literature procedure.[13] 4-Bromophenol, 4-Bromobenzaldehyde, Octyl cyanoacetate, Piperidine, 4-Bromobenzoic acid, 1-Octanol, Potassium carbonate, Tetrabutylammonium hexafluorophosphate, Triethylene glycol monomethyl ether, *N,N'*-Dicyclohexylcarbodiimide, 4-(Dimethylamino)pyridine, *N,N*-Dimethylacetamide, Pd(OAc)₂ and Pivalic acid were purchased from Sigma Aldrich and used without further purification.

2.2 Instrumentation

^{1}H and ^{13}C NMR spectra were recorded in Bruker NB 400 MHz using CDCl$_3$ as the solvent and tetramethylsilane (TMS, d = 0) as the internal standard. Molecular weights of small molecules were confirmed using Matrix-assisted laser desorption and ionization (MALDI) mass spectra were recorded on a Bruker ultraflextreme MALDI-mass spectrometer by using 4-HCCA (a-hydroxycinnamic acid) matrix. Thermal stability were analyzed using Mettler TOLEDO TGA/SDTA 851e at a heating rate of 10° C/min. X-ray diffraction (XRD) data of small molecules were obtained using Bruker AXS D8 Advance X-ray diffractometer. Cu Kα wavelength was used for XRD experiments. Differential scanning calorimetry was performed using DSC Q100 (TA Instruments). DSC curves were recorded at a scanning rate of 10°C min under a nitrogen flow. Electrochemical analysis were performed by cyclic voltammetry using CH instruments, CHI 600D electrochemical work station with platinum disc as working electrode, Ag/AgCl as reference electrode and platinum wire as counter electrode. The experiments were carried out by coating a thin layer of small molecules in platinum disc electrode and measurements were taken in 0.1M Tetrabutylammonium hexafluorophosphate as supporting electrolyte. UV-vis-NIR absorption spectra were recorded using Varian Carey 50 Bio UV–visible spectrophotometer. For solid state, spin coating was done on quartz from solution in chloroform with a concentration of 1mg ml^{-1}.

2.3 Theoretical Calculations

Density functional theory (DFT) calculations were performed using the Gaussian 09 ab initio quantum chemical software package.[14] The ground state geometries of all the molecules were optimized in gas phase using the hybrid Becke's three-parameter gradient-corrected functional (B3LYP) [15] along with 6-31G(d) basis set. The B3LYP functional has been proved to be reliable for its optimum prediction of properties for DPP based systems.[16] Frequency calculations were performed at the same level of theory to check for consistency in the optimized geometries. The excited state properties of the systems were calculated using the time dependent-DFT theory (TD-DFT) using the hybrid PBE exchange correlational functional (PBE0) [17] in combination with the 6-31G(d) basis set. Single-point TD-DFT calculations for the first 20 singlet-singlet vertical transitions were carried out using the optimized geometries of the systems. The solvent environment was incorporated using the polarizable continuum solvation model (PCM) with chloroform as solvent.[18]

Journal Name **ARTICLE**
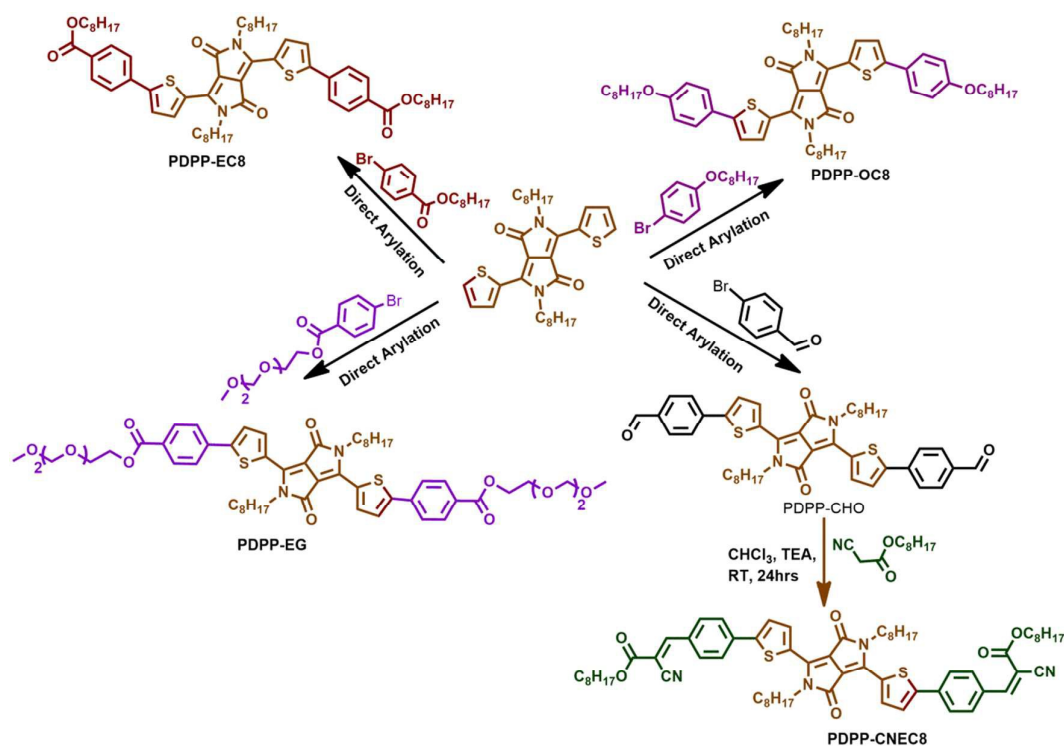
Scheme 1. Synthetic strategy for four small molecules

2.4 Mobility Measurements

Device fabrication

Hole only device of the small molecules were fabricated on patterned ITO coated glass substrate. After patterning, the substrates were thoroughly washed with soap solution. Then substrates were ultrasonicated in deionised water for 15 minutes. As a final cleaning step, substrates were boiled in RCA solution for 15 minutes and then ultrasonicated in deionised water for 15 minutes. RCA solution is a mixture of H_2O_2 : NH_4OH : H_2O in the proportion of 1:1:5. After drying the substrates with nitrogen gun, PEDOT:PSS was spin coated. PEDOT:PSS solution was prepared by mixing 2 parts water to 1 part PEDOT:PSS followed by filtering the solution with 0.45 micron filter and then spin coated at 1000 RPM for 60 seconds. Spin coated PEDOT:PSS was annealed at 120^oC for 20 minutes. After letting the substrate cool at room temperature, active material was spin coated. Active material solution was prepared in chloroform with concentration of 10mg/ml and solution was stirred on a magnetic stirrer for 4 hours. Solutions were filtered with 0.45 micron filter and then spin coated at 1000 RPM for 60 seconds. The Gold (Au) electrode was deposited by thermal evaporation under a vacuum of 10^{-5} millibar. Initial deposition rate was 0.1 A/s and after depositing 15 nm of electrode, rate was slowly increased under a vacuum of 10^{-5} millibar. Initial deposition rate was 0.1 A/s and after depositing

15 nm of electrode, rate was slowly increased to 1 A/s and after 50 nm, rate was increased to 5 A/s. Mobility was calculated by fitting the SCLC model to the I-V characteristics from the following equation.

$$J = \frac{9}{8}\mu\varepsilon_0\varepsilon_r \frac{(V - V_{bi})^2}{d^3}$$

where J is the current density, d is the film thickness of active layer, μ is the hole mobility, ε_r is the relative dielectric constant of the transport medium, ε_0 is the permittivity of free space (8.85×10^{-12} Fm^{-1}), V is the voltage applied and V_{bi} accounts for various barriers in the device. The V_{bi} can be determined from the transition between the ohmic region and the SCLC region.

3. Results and Discussion

3.1 Synthesis

The targeted four small molecular structures are displayed in Figure 1 and their synthetic routes are shown in Scheme 1. All the molecules were synthesized using direct arylation under ligand free condition using 3 equiv K_2CO_3, 33 mol % pivalic acid (PivOH), 5 mol % Pd(OAc)$_2$ and anhydrous dimethylacetamide (DMA) at 110 °C for 16 h to achieve the target small molecules **PDPP-EC8**, **PDPP-EG**, **PDPP-OC8** and **PDPP-CHO** in yields of 57%, 61%, 58% and 47%. Coupling or branching defect was observed in Maldi even after purification with column chromatography.[19] All the four small molecules were carefully purified using recrystallisation thrice with ethylacteate .The final molecular structures of
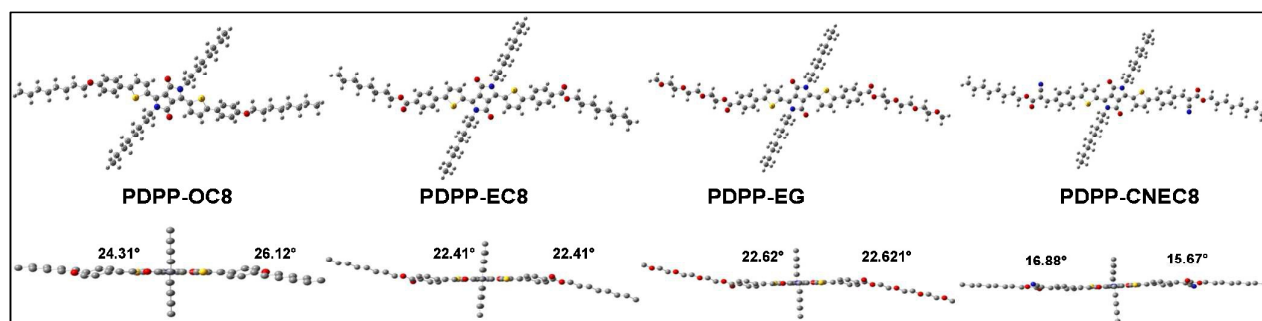
Journal Name

ARTICLE

Figure 2. Optimized structures of the small molecules at B3LYP/6-31G(d) level of theory and their corresponding dihedral angles.

the systems were confirmed by ^{1}H-NMR, ^{13}C-NMR and MALDI-TOF (for spectra see SI). The synthesized molecules exhibit good solubility in common organic solvent such as chloroform, tetrahydrofuran, chlorobenzene and dichlorobenzene.

3.2 Geometry

The optimized geometries from the DFT calculations along with dihedral angles of each molecule are displayed in Figure 2. It can be noted that the calculated dihedral angles of the molecules vary between 15° to 26° degrees. Also, the systems **PDPP-EC8** and **PDPP-EG** are showing almost similar conformational twists (≈23°) along the backbone. The introduction of the **PDPP-CNEC8** unit induces less conformational twist in the order of ≈16° when compared to other systems. This may be due to the limitations induced to the steric twisting by the vinylene double bond. Among the four molecules, **PDPP-OC8** shows the larger torsions of about ≈26°. These results elicit the influence of various side chains on the backbone planarity of the molecule and thereby affecting the inter-molecular packing and conjugation of the system.

3.3 Optical properties

The ultraviolet/visible (UV/vis) absorption spectra for the four small molecules in dilute chloroform solution and spin coated thin film are shown in Figure 3. Their corresponding optical parameters are listed in Table 1. All the molecules exhibit two distinct absorption bands at shorter and longer wavelength regions attributed to π-π* and internal charge transfer. Such absorption profile reflects the typical donor–acceptor π-conjugated system.[20] Compared to solution all the molecules exhibit red shifts in both shorter and long wavelength regions in thin film. This is due to strong intermolecular π–π stacking in solid state. The optical band gap in solid state derived from the onset of absorption spectra decreases in the order of **PDPP-OC8** > **PDPP-EC8** ≈ **PDPP-EG** > **PDPP-CNEC8**, with decrease
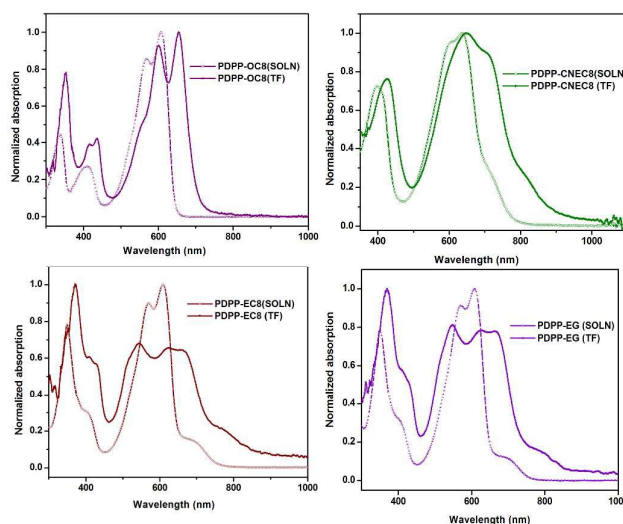

Figure 3. Normalized UV-vis absorption spectra of **PDPP-OC8**, **PDPP-CNEC8**, **PDPP-EC8** and **PDPP-EG** in chloroform and in film.

in E_g (by ca. 0.1–0.2 eV). It is noteworthy that **PDPP-CNEC8**, **PDPP-EG** and **PDPP-EC8** exhibit a broad absorption covering solar spectrum in the range of 500 to 800 nm. Specifically ~120 nm red shift is observed in the onset of absorption (λ_{onset}) when replacing the alkoxy side chain by electron-withdrawing ester substituent side chain their optical band gap in thin film is reduced from 1.65 to 1.43eV. The absorption maxima (λ_{max}) also show red shift in both solution and thin film when replacing alkoxy to ester. This may be due to strong π-intermolecular interaction in solid state. Particulary electron withdrawing side chain substituted molecules **PDPP-EG PDPP-CNEC8** and **PDPP-EC8** shows a discernible vibronic shoulder attributed to molecular rigidity and aggregating nature in solid state[7,21,22] whereas **PDPP-OC8** with alkoxy side chain exhibit narrower absorption and sharp onset. The TD-DFT results

substantiate experimental results and the absorption profiles of the molecules extend over a broad range from ≈300 to 700 nm. The dominant lower energy band (≈600 to 700 nm) transitions of the systems are the intra-molecular charge transfer absorption peaks which mainly arise from HOMO → LUMO transitions. Each system exhibit another important peak at the high energy band (≈300 to 400 nm) of π-π* nature with HOMO-2 → LUMO transitions. The simulated absorption spectra of the systems elicit that changing the terminal end groups from **PDPP-OC8** to **PDPP-CNEC8** results in bathochromic shift of the absorption maxima from ≈600 to 690 nm. It is important to note that the molecule **PDPP-CNEC8** exhibit the maximum red-shifted absorption
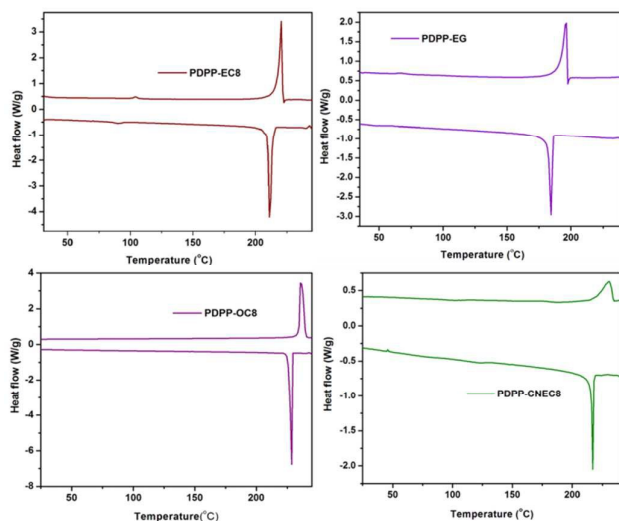

Figure 4. DSC scans of **PDPP-EC8**, **PDPP-CNEC8**, **PDPP-OC8** and **PDPP-EG**

at about ≈690 nm. Analysing the electron density contours of the small molecular systems is significant to understand the nature of
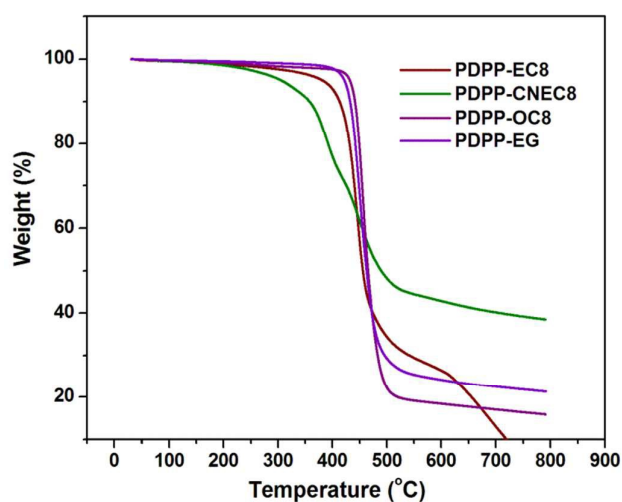

Figure 5. TGA plots of **PDPP-EC8**, **PDPP-CNEC8**, **PDPP-OC8** and **PDPP-EG** at a heating rate of 10 °C min⁻1 in an inert atmosphere

their transitions. In all the molecules, the HOMOs are delocalized mainly on the central thienyl DPP unit whereas the LUMOs extend from DPP to phenyl fragment except **PDPP-OC8**. This is because of the electron withdrawing nature of side chain.
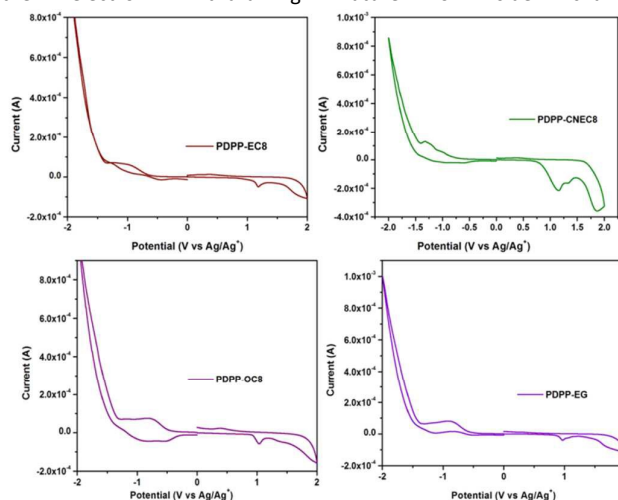

Figure 6. Cyclic voltammograms for small molecules in 0.1 M Bu_4NPF_6 acetonitrile solution at the rate of 0.1 Vs^{-1}, with Ag–AgCl as the reference electrode.

3.4 Thermal properties

In order to analyze the thermal transition of the four donor small molecules, Differential Scanning Calorimetry (DSC) was performed and the results are depicted in Figure 4. Their melting and crystallization temperatures are presented in Table 1. The melting temperatures (T_m) of **PDPP-EC8**, **PDPP-EG**, **PDPP-CNEC8** and **PDPP-OC8** are 227, 197, 229 and 236 °C respectively and their corresponding crystallizing temperatures (T_c) are of 209, 185, 215 and 225 °C. Among the four molecules, **PDPP-OC8** exhibits high melting and crystallization temperature which indicates their rigid solid packing. Compared to **PDPP-EC8**, **PDPP-EG** exhibits low melting and crystallization temperature due to the high flexible nature of the glycol chain.[23] PDPP-EC8 exhibit double transition 221 and 104°C probably due to liquid crystal nature and these behavior are not shown for other three molecules because of the nature of flexible side chain to the conjugated core which essential for LC behavior may reduced.[24] Thermal behavior of small molecules have been further investigated using Thermogravimetric analysis (TGA) as shown in Figure 5 and their corresponding decomposition temperatures were listed in Table 1. All the small molecules possess good thermal stability with decomposition temperatures greater than 300 °C (5% weight loss) under N_2 atmosphere.

3.5 Electrochemical Properties

In order to understand the electronic energy levels of small molecules, cyclic voltammetry has been carried out. The highest occupied molecular orbital (HOMO) and lowest unoccupied molecular orbital (LUMO) can be estimated from the onset of

oxidation and reduction potential which correspond to ionization   potential (IP) and electron affinity (EA) of small molecules.

Table.1 Optical, electrochemical and thermal properties of **PDPP-OC8**, **PDPP-EC8**, **PDPP-EG** and **PDPP-CNEC8**

Small molecule	λ_{max}(nm)		λ_{edge}(nm)[c] (thin film)	E_g^{opt} (eV)[d]	E_{HOMO} (eV)[e]	E_{LUMO} (eV)[e]	E_g^{elc} (eV)[f]	DSC		TGA
	Solution[a]	Thin film[b]						T_m (°C)[g]	T_c (°C)[h]	T_d (°C)[i]
PDPP-OC8	341,410,569,609	352,411,434,599,654	751	1.65	-5.31	-3.62	1.69	236	225	434
PDPP-EC8	350,569,609	371,547,623,661	865	1.43	-5.36	-3.82	1.54	227	209	381
PDPP-EG	351,571,611	370,548,629,666	867	1.43	-5.28	-3.76	1.52	197	185	418
PDPP-CNEC8	397,603,635	426,646,711	877	1.41	-5.24	-3.74	1.50	229	215	303

[a]Absorption spectra recorded in $CHCl_3$ solution (1.0×10^{-5}M). [b]Spin coated on $CHCl_3$ solution (1 mg/ml) on quartz plate. [c]Onset of absorption in thin film. [d]Optical band gap calculated using the formula $E_g^{opt}=1240/\lambda_{edge,film}$. [e]Calculated according to the formula $E_{HOMO/LUMO} = -e(E_{ox/red} + 4.41)$ (eV). [f]$E_g^{elc}= E_{LUMO}-E_{HOMO}$. [g]$T_m$ = melting temperature. [h]T_c = Crystallization temperature. [i]T_d = decomposition temperature.
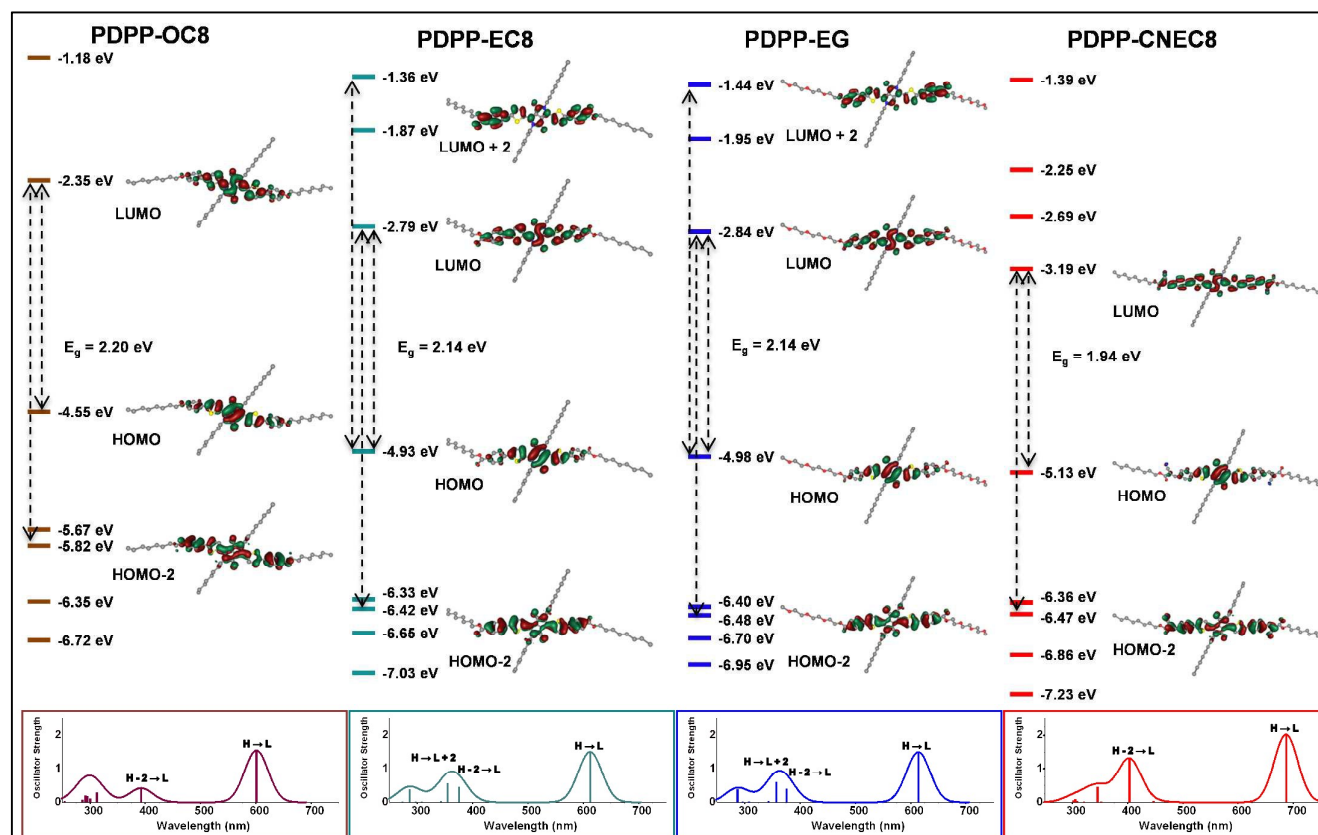

Figure 7. Electron density plots of FMOs (H atoms are not shown for clarity), optical transitions and oscillator strengths of the four small molecules calculated using DFT B3LYP/6-31G(d) and TD-DFT PBE1PBE/6-31G(d) levels of theory.

Cyclic voltammogram of small molecules in thin film are displayed in Figure 6 and their electrochemical parameters are shown in Table 1. From the oxidation and reduction onset values, the HOMO and LUMO levels can be calculated with respect to ferrocene standard by the following eqn.[25]

HOMO = −IP = − (E_{ox} + 4.41) (eV)   (1)

LUMO = −EA = − (E_{red} + 4.41) (eV)   (2)

The electrochemical band gaps calculated from the above equation are in good agreement with optical band gaps. From the figure 6 all the four molecules exhibit irreversible oxidation and reduction wave and the similar redox process was also observed for other dpp based molecular system.[26] Specifically, the HOMO energy level of both **PDPP-OC8** (-5.31 eV) and **PDPP-EC8** (-5.36 eV) are similar, however much variation is noticed in LUMO energy level of **PDPP-OC8** (-3.62 eV) to **PDPP-EC8** (-3.82 eV). This clearly enlighten the electron-withdrawing ester effect in **PDPP-EC8.** This effect

Journal Name   **ARTICLE**

significantly lowers the LUMO level for **PDPP-EC8** and **PDPP-EG** which reduces the band gap. The frontier molecular orbitals of the four systems were calculated using DFT and compared with the experimental CV results. The calculated energy levels of the small molecules are shown in the Figure 7. Although DFT calculations have limitations in accuracy of the predicted molecular energy levels, the trends in variations of these energy levels can be reliable. The theoretical results show that the HOMO and LUMO energy levels are consistent with the experiment. It can be observed from these energy levels that the HOMO energies range from -4.55 to -5.13 eV while the LUMOs range between -2.35 and -3.19 eV. The energy gaps of the various side chain functionalized small molecules are in the order **PDPP-OC8 > PDPP-EG ≈ PDPP-EC8 > PDPP-CNEC8**. It is interesting to see that the glycol and the alkoxy functionalized systems show similar energy levels. These results indicate that the system **PDPP-CNEC8** maintains a low energy gap among the four candidates.

3.6 X-Ray diffraction (XRD)

In order to understand the packing nature of the small molecules thin film X-ray diffraction (XRD) was performed in thin film, spin coated from glass substrate. The XRD patterns of four small molecules are displayed in Figure 8. All the four small molecules exhibit first order diffraction peak at 2Θ=4.76 for **PDPP-OC8**, 2.96 for **PDPP-EC8**, 3.08 for **PDPP-EG** and 3.44 for **PDPP-CNEC8** corresponding to d–spacing values of 18.33, 29.62, 28.52 and 25.67 Å, respectively which attribute to interchain ordering. From the figure it is clear that, **PDPP-OC8** exhibit second order diffraction peak at 2Θ=9.20, 13.80 which correspond to the d values of 9.63 and 6.42 Å attributed to side chain ordering and the third order diffraction peak at 2Θ=18.50 correspond to 4.81 Å attributed to intermolecular d spacing.[22,27] From the above result, it was clear that **PDPP-OC8** exhibit highly ordered organization in the solid state.

3.7 Hole mobility

The hole mobility of the pristine small molecules were measured using space charge limited current (SCLC) method with the device structure of ITO/ PEDOT: PSS/small molecule/ Au and their SCLC curve were shown in Figure 9. The hole motilities of **PDPP-OC8**, **PDPP-EC8**, **PDPP-EG** and **PDPP-CNEC8** were estimated as 1.26×10^{-4} $cm^2 V^{-1} s^{-1}$, $7.17 \times 10^{-6} cm^2 V^{-1} s^{-1}$, $2.69 \times 10^{-5} cm^2 V^{-1} s^{-1}$ and $1.03 \times 10^{-5} cm^2 V^{-1} s^{-1}$ respectively. Compared to **PDPP-EC8**, **PDPP-EG**, **PDPP-CNEC8**, the hole mobility of **PDPP-OC8** improved by two order of magnitude probably due to the electron donating nature of alkoxy group which was differ from the other three (electron withdrawing substitution).The results were also well correlated with XRD as discussed above.
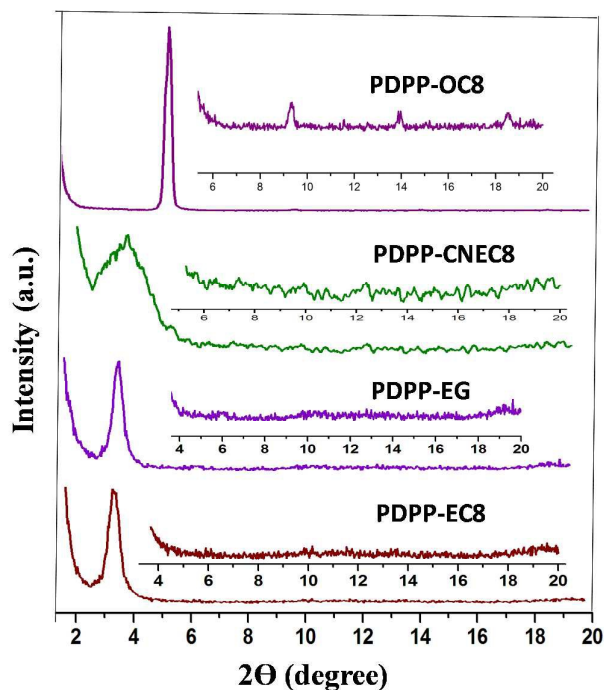

Figure 8. XRD traces of **PDPP-OC8**, **PDPP-EC8**, **PDPP-EG** and **PDPP-CNEC8**.
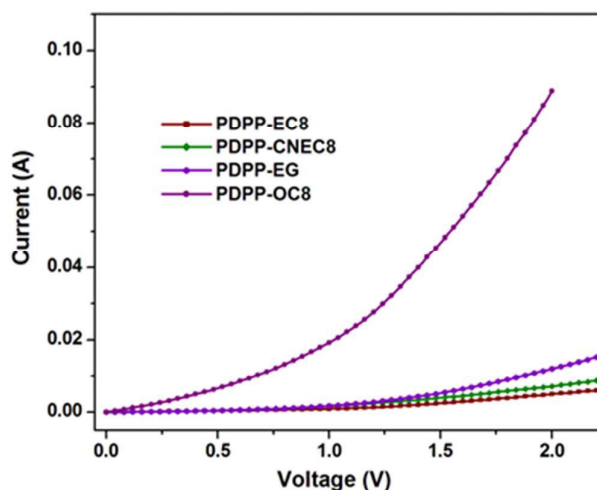
Figure 9. Current vs voltage characteristics of hole only device of small molecules.

4. Conclusion

In Conclusion, we successfully synthesized a series of DPP based small molecules using direct arylation methodologies. The four small molecules were confirmed by NMR and MALDI-TOF MS. A comprehensive study has been performed using absorption spectroscopy, cyclic voltammetry, XRD and hole mobility in order to analysis how the functional side chain substitution impact on optical, HOMO, LUMO, band gap and device performance. We find

ARTICLE

Journal Name

that a simple replacement of alkoxy group from ester leads a drastic change in their absorption profile (by ≈0.2 eV and 120 nm red shift on onset) enlighten the effect of electron withdrawing nature of terminal position. Of all the four molecules **PDPP-OC8** exhibits high carrier mobility, due to highly ordered structure and strong intermolecular interaction which was clearly supported by XRD data. The theoretical calculations provide more insights regarding the nature of the small molecules. The simulated absorption spectra and the charge density plots reveal the effect of side chains in the optical properties of the molecules. We have also identified a coupling defect occur in thienyl DPP and conveniently identified by Maldi –mass. Thus a basic understanding on the selectivity of C-H monomer in direct arylation has yet to be carefully understood and proper optimization on reaction condition is the essential tool for assuring the reaction yield and purity.

Acknowledgements

References

1   A. J. Heeger, *Adv. Mater.,* 2014, **26**, 10; (c) C. J. Brabec, M. Heeney, I. McCulloch and J. Nelson, *Chem. Soc. Rev.,* 2011, **40**, 1185; (c) B. C. Thompson and J. M. J. Frechet, *Angew. Chem.,* 2008, 47, 58; (d) N. Espinosa, M. Hosel, M. Jørgensen and F. C. Krebs, *Energy Environ. Sci.*, 2014, **7**, 855; (e) K. A. Mazzio and C. K. Luscombe, *Chem. Soc. Rev.*, 2015, **44**, 78.

2   T. L. Nguyen, H. Choi, S.J. Ko, M. A. Uddin, B. Walker, S. Yum, J. E. Jeong, M. H. Yun, T. J. Shin, S. Hwang, J. Y. Kim and H. Y. Woo, *Energy Environ. Sci.*, 2014, **7**, 3040; (b) Y. Liu, J. Zhao, Z. Li, C. Mu, W. Ma, H. Hu, K. Jiang, H. Lin, H. Ade and H. Yan, *Nat. Commun.*, **5**, 5293; (c) N. Li, D. Baran, G. D Spyropoulos, H. Zhang, S. Berny, M. Turbiez, T. Ameri, F. C. Krebs and C. J. Brabec, *Adv. Energy Mater.,* 2014, **4**, 1400084; (d) C. C. Chen, W. H. Chang, K. Yoshimura, K. Ohya, J. You, J. Gao, Z. Hong and Y. Yang, *Adv. Mater.*, 2014, **26,** 5670; (e) J. You, L. Dou, K. Yoshimura, T. Kato, K. Ohya, T. Moriarty, K. Emery, C. C Chen, J. Gao, G. Li and Y. Yang, *Nat. Commun.,* 2013, **4**, 1446.

3   W. Ni, X. Wan, M. Li, Y. Wang and Y. Chen, *Chem. Commun.,* 2015, **51,** 4936; (b) Y. Sun, G. C. Welch, W. L. Leong, C. J. Takacs, G. C. Bazan and A. J. Heeger, *Nat. Mater.,* 2012, **11,** 44.

4   Q. Zhang, B. Kan, F. Liu, G. Long, X. Wan, X. Chen, Y. Zuo, W. Ni, H. Zhang, M. Li, Z. Hu, F. Huang, Y. Cao, Z. Liang, M. Zhang, T. P. Russell and Y. Chen1, *Nat. Photon.,* 2014, **9**, 35; (b) B. Kan, M. Li, Q. Zhang, F. Liu, X. Wan, Y. Wang, W. Ni, G. Long, X. Yang, H. Feng, Y. Zuo, M. Zhang, F. Huang, Y. Cao, T. P. Russell and Y. Chen, *J. Am. Chem. Soc.,* 2015, **137**, 3886; (c) B. Kan, Q. Zhang, M. Li, X. Wan, W. Ni, G. Long, Y. Wang, X. Yang, H. Feng, and Y. Chen, *J. Am. Chem. Soc.,* 2014, **136**, 15529; (d) K. Sun, Z. Xiao, S. Lu, W. Zajaczkowski, W. Pisula, E. Hanssen, J. M. White, R. M. Williamson, J. Subbiah, J. Ouyang, A. B. Holmes, W. W.H. Wong and D. J. Jones, *Nat. Commun.,* **6,** 6013; (e) Y. Liu, C. C Chen, Z. Hong, J. Gao, Y. M. Yang, H. Zhou, L. Dou, G. Li and Y. Yang, *Sci. Rep.,* **3**, 3356.

5   L. Fu, W. Fu, P. Cheng, Z. Xie, C. Fan, M. Shi, J. Ling, J.Hou, X. Zhanc and H. Chen, *J. Mater. Chem. A,* 2014, **2**, 6589; (b) J.

Liu, Y. Sun, P. Moonsin, M. Kuik, C. M. Proctor, J. Lin, B. B. Hsu, V. Promarak, A. J. Heeger, T. Q. Nguyen, *Adv. Mater.,* **2013**, *25*, 5898; (c) S. Qu and H. Tian, *Chem. Commun.,* 2012, **48**, 3039.

D. J. Schipper and K. Fagnou, *Chem. Mater.,* 2011, **23**, 1594; (b) D. J. Burke and D. J. Lipomi, *Energy Environ. Sci.,* 2013, **6**, 2053; (c) A. Facchetti, L. Vaccaro and A. Marrocchi, *Angew. Chem. Int. Ed.*, 2012, **51**, 3520; (d) L. G. Mercier and M. Leclerc, *Acc. Chem. Res.,* 2013, **7,** 1597.

6   S. Y. Liu, M. M. Shi, J. C. Huang, Z. N. Jin, X. L. Hu, J. Y. Pan, H. Y. Li, A. K. Y. Jen and H. Z. Chen, *J. Mater. Chem. A*, 2013, **1**, 2795. (b) S. Y. Liu, W. Q. Liu, J. Q. Xu, C. C. Fan, W. F. Fu, J. Ling, J. Y. Wu, M. M. Shi, A. K. Y. Jen and H. Z. Chen, *ACS Appl. Mater. Interfaces,* 2014, **6**, 6765. (c) S. Y. Liu, W. F. Fu, J. Q. Xu, C. C. Fan, H. Jiang, M. Shi, H. Y. Li, J. W. Chen, Y. Cao, and H. Z. Chen, *Nanotechnology*, 2014, **25,** 014006.

7   A. D. Hendsbee, J. P. Sun, L. R. Rutledge, I. G. Hill and G. C. Welch, *J. Mater. Chem. A*, 2014, **2**, 4198.

8   J. Areephong, A. D. Hendsbee and Gregory C. Welch, *New J. Chem,* 2015, *New J. Chem.*, 2015, **39**, 6714; (b) S. M. McAfee, J. M. Topple, A. J. Payne, J. P. Sun, I. G. Hill and G. C. Welch, *CHEMPHYSCHEM*, 2015, **16**,1190; (c) A. D. Hendsbee, S. M. McAfee, J. P. Sun, T. M. McCormick, I. G. Hill and G. C. Welch, *J. Mater. Chem. C*, 2015, **3**, 8904; (d) S. M. McAfee, J. M. Topple, J. P. Sun, I. G. Hill and G. C. Welch, *RSC Adv*., 2015, **5**, 80098; (e) S. M. McAfee, , J. S. J. McCahill, C. M. Macaulay, A. D. Hendsbee, and G. C. Welch, *RSC Adv*., 2015, **5**, 26097.

9   M. T. Lloyd, J. E. Anthony and G. G. Malliaras, *Materials Today.,* 2007, **10**, 34; O. P. Lee, A. T. Yiu, P. M. Beaujuge, C. H. Woo, T. W. Holcombe, J.E. Millstone , J. D. Douglas , M. S. Chen, and J. M. J. Fréchet, *Adv. Mater.,* 2011, **23**, 5359–5363

10 J. Mei and Z. Bao, *Chem. Mater.*, 2014, **26**, 604; (b) M. A. Naik, N. Venkatramaiah, C. Kanimozhi and Satish Patil, *J. Phys. Chem. C*, 2012, **116**, 26128; (c) K. H. Kim, H. Yu, H. Kang, D. J. Kang, C. H. Cho, H. H. Cho, J. H. Oh and B. J. Kim, *J. Mater. Chem. A*, 2013, **1**, 14538; (d) V. S. Gevaerts, E. M. Herzig, M. Kirkus, K. H. Hendriks, M. M. Wienk, J. Perlich, P. M. Buschbaum and R. A. J. Janssen, *Chem. Mater.*, 2014, **26**, 916.

11 (a) H. Song, Y. Gao, W. Li, H. Tian, D. Yan, Y. Geng and F. Wang, *J. Mater. Chem. C*, 2015, **3**, 11135. (b) C. Kanimozhi, N. Y-. Gross, E. K. Burnett, A. L. Briseno, T. D. Anthopoulos, U. Salznerd and S. Patil, *Phys. Chem. Chem. Phys.*, 2014, **16**, 17253. (c) Y. Li, C-.Y. Chang, Y. Chen, Y. Songa, C-.Z. Li, H-. L. Yip, A. K-.Y. Jen and C. Li, *J. Mater. Chem. C*, 2013, **1**, 7526.

12 A. B. Tamayo, X. D. Dang, B. Walker, J. Seo, T. Kent and T. Q. Nguyen, *Appl. Phys. Lett.,* 2009, **94,** 103301.

13 M. J. Frisch, G. W. Trucks, H. B. Schlegel, G. E. Scuseria, M. A. Robb, J. R. Cheeseman, G. Scalmani, V. Barone, B. Mennucci and G. A. Petersson, et al., Gaussian 09, Revision A.02, Gaussian, Inc., Wallingford, CT, 2009.

14 (a) A. D. Becke, J. Chem. Phys., 1993, 98, 5648–5652; (b) A. D. Becke, J. Chem. Phys., 1996, **104**, 1040–1046. (c) C. T. Lee, W. T. Yang and R. G. Parr, *Phys. Rev. B: Condens. Matter Mater. Phys.*, 1988, **37**, 785.

15 (a) A. Riano, P. M. Burrezo, M. J. Mancheno, A. Timalsina, J. Smith, A. Facchetti, T. J. Marks, J. T. Lopez Navarrete, J. L. Segura, J. Casado and R. P. Ortiz, *J. Mater. Chem. C*, 2014, **2**, 6376. (b) C-. L. Wang, J. Wang, F-. Q. Bai, J. Chen and H-. X. Zhang, Int. J. Quant. Chem. 2014, **114**, 560.

16 (a) J. P. Perdew, K. Burke, and M. Ernzerhof, *Phys. Rev. Lett.*, 1996, **77**, 3865. (b) J. P. Perdew, K. Burke, and M. Ernzerhof, *Phys. Rev. Lett.*, 1997, **78**, 1396. (c) C. Adamo and V. Barone, *J. Chem. Phys.*, 1999, **110**, 6158.

17 C. Bernini, L. Zani, M. Calamante, G. Reginato, A. Mordini, M. Taddei, R. Basosi, and A. Sinicropi *J. Chem. Theory Comput.*, 2014, **10**, 3925.

Journal Name

ARTICLE

18 C. Bernini, L. Zani, M. Calamante, G. Reginato, A. Mordini, M. Taddei, R. Basosi, and A. Sinicropi *J. Chem. Theory Comput.*, 2014, **10**, 3925.

19 J. Kudrjasova, J. Kesters, P. Verstappen, J. Brebels, T. Vangerven, I. Cardinaletti, J.Drijkoningen, H. Penxten, J. Manca, L. Lutsen, D. Vanderzandeab and W. Maes, *J. Mater. Chem. A*, 2016, **4**, 791.

20 A. B. Tamayo, B. Walker and T. Q. Nguyen, *J. Phys. Chem. C*, 2008, **112**, 30.

21 J. W. Lee, Y. S. Choi and W. H. Jo, *Organic Electronics.,* **13**, 2012, 3060.

22 D. Qian, B. Liu, S. Wang, S. Himmelberger, M. Linares, M. Vagin, C. Muller, Z. Ma, S. Fabiano, M. Berggren, A. Salleo, O. Inganas, Y. Zouf and F. Zhang, *J. Mater. Chem. A*, 2015, 3, 24349

23 J. E. Donaghey, A. Armin, P. L. Burn and P. Meredith, *Chem. Commun.*, 2015, **51**, 14115.

24 C. Kim, J. Liu, J. Lin, A. B. Tamayo, B. Walker, G. Wu and T. Q. Nguyen, *Chem. Mater*., 2012, **24**, 1699.

25 P. Shen, H. Bin, L. Xiao, and Y. Li, *Macromolecules*., 2013, **46**, 9575.

26 S. Loser, C. J. Bruns, H. Miyauchi, R. P. Ortiz, A. Facchetti, S. Stupp and T. J. Marks,*J. Am. Chem. Soc*., 2011, **133**, 8142; Y. Lin, L. Ma, Y. Li, Y. Liu , D. Zhu and X. Zhan, *Adv. Energy Mater*., 2013, **3**, 1166.

27 H. Jia, L. Li, Z. Lu, W. Zhang, W. He, B. Jiang, A. Tang, Z. Tan, C. Zhan, Y. Li and J. Yao, *Phys. Chem. Chem. Phys*., 2012, **14**, 14238; J. Huang, C. Zhan, X. Zhang, Y. Zhao, Z. Lu, H. Jia, B. Jiang, J. Ye, S. Zhang, A. Tang, Y. Liu, Q. Pei and J. Yao, *ACS Appl. Mater. Interfaces*., 2013, **5**, 2033.

New Journal of Chemistry Accepted Manuscript

Structure-properties relationship in diketopyrrolopyrrole based small molecules using functional terminal side chains via direct arylation: a joint experimental and theoretical study

B. Sambathkumar,[ab] P. Shyam Vinod Kumar ,[ab] K. Saurav,[c] S. Sundar Kumar Iyer,[c] V. Subramanian,[ab] and

N. Somanathan*[ab]

The role of terminal side chain on diketopyrrolopyrrole based small molecules has been analyzed and it provides how their optoelectronic properties vary according to their side chain nature.